The resonant population of asteroids in librating states of the ν 6 linear secular resonance

M Huaman, F. Roig, V Carruba, R C Domingos, Safwan Aljbaae

The resonant population of asteroids in librating states of the ν_6 linear secular resonance

M. Huaman,[1,2]⋆ F. Roig,[1] V. Carruba,[2] R. C. Domingos[3] and S. Aljbaae[2]

[1] *Observatório Nacional (ON), Rua Gal. Jose Cristino 77, Rio de Janeiro RJ 20921-400, Brazil*
[2] *São Paulo State University (UNESP), School of Natural Sciences and Engineering, Guaratinguetá SP 12516-410, Brazil*
[3] *São Paulo State University (UNESP), Campus of São João da Boa Vista SP 13876-750, Brazil*

ABSTRACT

We discuss the asteroid population evolving close by or into the ν_6 secular resonance in the main asteroid belt. Using the analytical method of Yoshikawa, we estimate the actual domain of the ν_6 resonance, which currently contains 4 137 asteroids identified from the AstDys catalogue. We perform numerical integrations of the obits of these asteroids, considering the gravitational perturbation of all the planets, and identify those showing pure libration states. For the first time, seven asteroids are found to librate in aligned states, all located at the central main belt. We analyse the stability of this new population by extending our numerical integrations both into the past and into the future, to find that all of them are stable, but only four of them display long-term aligned librations. We also identified the asteroid families located close to and within the domain of the ν_6 secular resonance, with a particular focus on the Svea family, which has 54 per cent of its members librating in anti-aligned states. This is the third family identified to be largely affected by the ν_6 resonance, together with the families of Tina and Euphrosyne.

Key words: celestial mechanics – minor planets, asteroids: general.

1 INTRODUCTION

The ν_5, ν_6, and ν_{16} linear secular resonances in the asteroid belt occur when there is a one-to-one commensurability between the frequency of precession of an asteroid's perihelion, g, or the frequency of regression of an asteroid's node, s, and the corresponding frequencies of either Jupiter, g_5, or Saturn, g_6, s_6. The ν_6 resonance, in particular, corresponds to the condition $g \approx g_6$. This resonance is of particular importance since it constitutes a major boundary for the distribution of asteroids in the main belt.

Tisserand (1882) and Charlier (1902) performed the first attempts to construct a secular theory of planetary motion using an expansion of the disturbing function to a high degree. Later on, Hagihara (1928) developed a high-order secular theory for Jupiter and Saturn, and Brouwer & van Woerkom (1950) improved the linear secular theory for the outer planets to accurately determine the values of the fundamental frequencies g_5, g_6, s_6. In this context, Williams (1969) used a non-linear analytical theory to study the secular evolution of asteroids perturbed by the giant planets, and suggested that the linear secular resonances ν_5, ν_6, ν_{16} are strong mechanisms of asteroid depletion. Yoshikawa (1987), Knežević et al. (1991), Morbidelli & Henrard (1991b), and Morbidelli (1993) studied in detail

the dynamics and topology of the phase space of the linear secular resonances from the Hamiltonian approach.

The dynamics of the ν_6 secular resonance is characterized by either the libration or the circulation of the resonant argument $\sigma_6 = \varpi - \varpi_6$, where ϖ is the longitude of the asteroid perihelion and ϖ_6 is that of Saturn. In a circulating state, σ_6 varies continuously from $0°$ to $360°$, while in a librating state the resonant argument is bounded to oscillate around an equilibrium point. Two equilibria are possible, one around $0°$ and another around $180°$. The libration around $0°$ is called an 'aligned libration', since in this configuration the two perihelia of the asteroid and the planet are roughly oriented in the same direction. On the other hand, the libration around $180°$ is called an 'anti-aligned libration'; this latter libration usually occurs when the orbit of the asteroid is closer to the orbit of the planet (Yoshikawa 1987). Morbidelli & Henrard (1991a) and Morbidelli (1993) described the ν_6 resonance as an atypical case among secular resonances, because the locus of the resonance is almost independent on the orbital eccentricity (i.e. the resonance occurs at a given distance from the Sun and a given orbital inclination, but for all values of the eccentricity; Williams & Faulkner 1981). Since a perihelion secular resonance pumps up the eccentricity while keeping the inclination approximately constant, a body evolving in the ν_6 resonance may in principle have its eccentricity growing indefinitely.
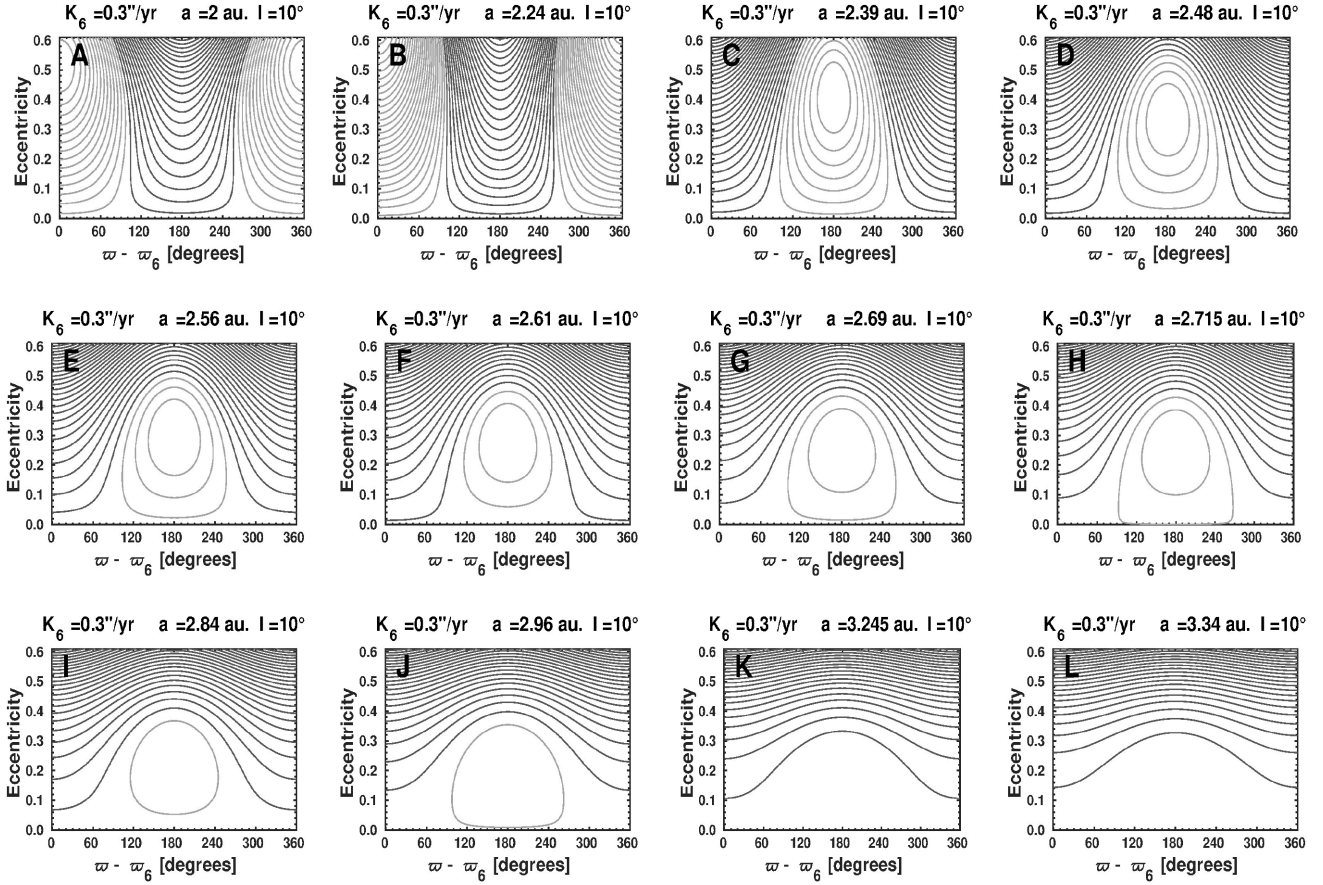

⋆ E-mail: mariet142@gmail.com

Figure 1. Level curves of the Hamiltonian model for the ν_6 secular resonance according to Yoshikawa (1987) and Morbidelli & Henrard (1991b) for $\sigma_6^* \to 0°$ (equation 2). The parameter $k_6 = 0.3$ arcsec yr^{-1} corresponds to $b - g_6$ (see text). The upper row panels give the phase portraits for four different values of a in the inner main belt. The middle row panels correspond to the central main belt, and the lower row panels to the outer main belt. Inclination is the same in all cases (10°). The dark and light grey colours identify the circulation and libration regimes, respectively. See text for discussion.

Numerical simulations by Froeschlé & Scholl (1993) allowed the identification of several comets and asteroids showing anti-aligned librations within the ν_6 resonance. The dynamical influence of this resonance on some asteroid families has been recently addressed by Carruba & Morbidelli (2011a), who identified the family of Tina with all of its members in anti-aligned libration. Besides, Machuca & Carruba (2012) and Carruba, Aljbaae & Souami (2014) found 19 members of the family of Euphrosyne also in anti-aligned libration. These bodies may represent a transient population that is temporarily captured in the resonance, or they may be members of a long-lasting group of resonant bodies.

In this work, we propose to extend the previous results by performing a global study of the dynamical evolution of real asteroids that interact with the ν_6 resonance. In Section 2, we apply the analytical method of Yoshikawa (1987) to estimate the possible boundaries of the resonance in terms of the orbital elements a, e, I (semi-major axis, eccentricity, and inclination, respectively) and of the frequency g. In Section 3, we present the results of the numerical simulations that allow the identification of those asteroids within the resonance boundaries that show pure libration states. The effects of the ν_6 resonance on the asteroid families are addressed in Section 4. Finally, Section 5 is devoted to the conclusions.

2 TOPOLOGY AND DOMAIN OF THE ν_6 SECULAR RESONANCE

The analytical model of Yoshikawa (1987) considers that the dynamics of the ν_6 resonance is approximately described by the following one degree of freedom Hamiltonian function:

$$F_{\nu_6} = \frac{1}{2}(b - g_6)\,e^2 + \frac{1}{4}c\,e^4 - d\,e\cos(\varpi - \varpi_6^*) \qquad (1)$$

where $\varpi_6^* = g_6 t + \text{const.}$, b is a coefficient that depends on a, I, and c, d are coefficients that depend only on a. The evolution of this Hamiltonian describes the changes in eccentricity and resonant argument, $\sigma_6^* = \varpi - \varpi_6^* \approx \sigma_6$, for different fixed values of the semi-major axis and inclination. The solutions of this Hamiltonian generate two different equilibrium points corresponding to the conditions $d\sigma_6^*/dt = 0$ and $de/dt = 0$: one equilibrium for $\sigma_6^* = 0°$ and the other for $\sigma_6^* = 180°$. Therefore, we can rewrite the Hamiltonian either as:

$$F'_{\nu_6}(\sigma_6^* \to 0°) = \frac{1}{2}(b - g_6)\,e^2 + \frac{1}{4}c\,e^4 - d\,e\cos(\sigma_6^*) \qquad (2)$$

or

$$F'_{\nu_6}(\sigma_6^* \to 180°) = \frac{1}{2}(b - g_6)\,e^2 + \frac{1}{4}c\,e^4 + d\,e\cos(\sigma_6^{*\prime}) \qquad (3)$$

where $\sigma_6^{*\prime} = \sigma_6^* + 180°$. According to Morbidelli & Henrard (1991b), equation (2) gives the characteristic evolution of
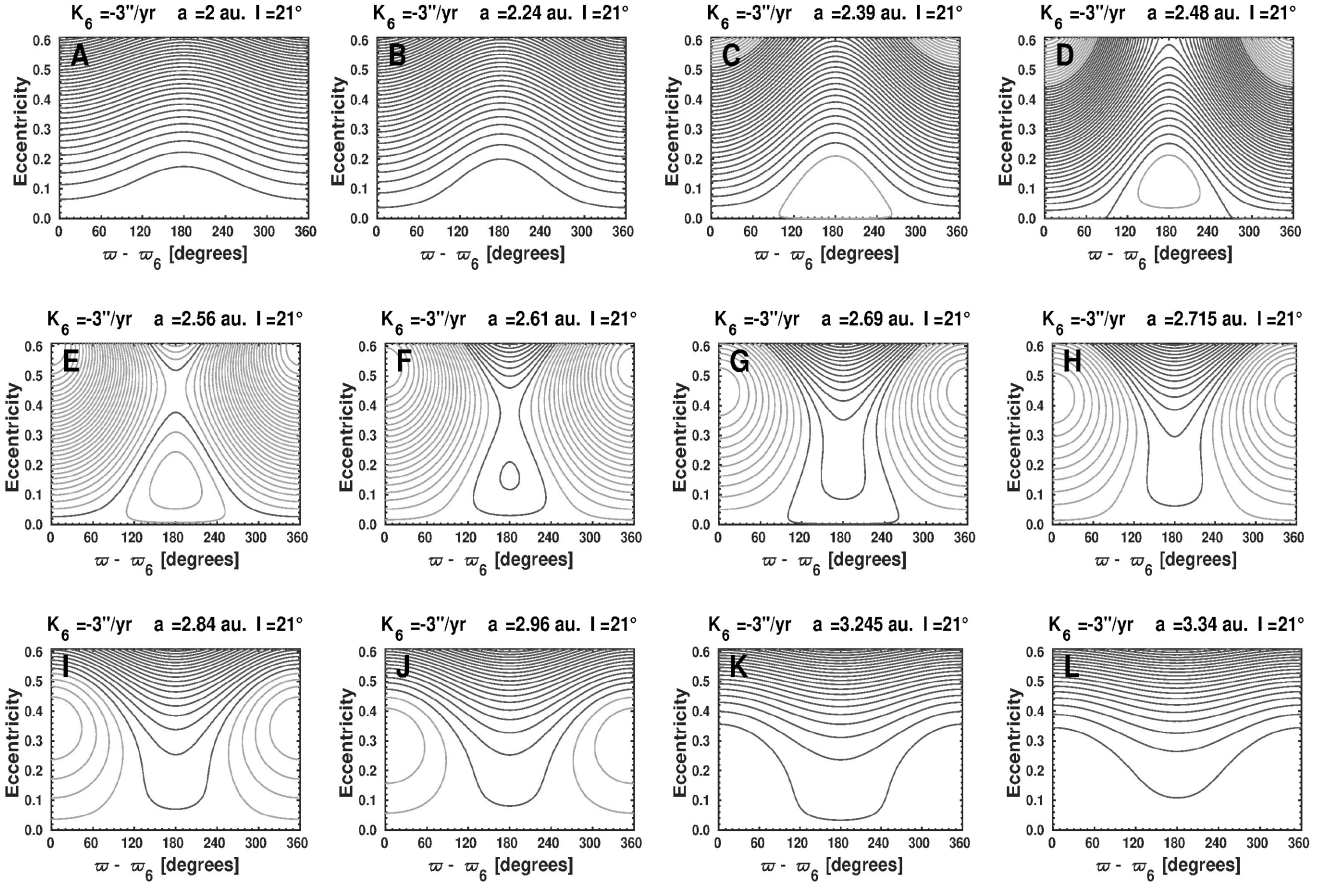
Figure 2. Same as Fig. 1, but for $\sigma_6^* \to 180°$ (equation 3), $k_6 = -3.0$ arcsec yr^{-1}, and inclination 21°.

Table 1. Ranges of the parameter $k_6 = b - g_6$ of the Yoshikawa (1987) analytical model that lead to libration of the critical argument, in terms of the location in the main asteroid belt. The first column gives the location in the semi-major axis, the second column gives the interval of k_6 where librations can occur, and the third and fourth column discriminate between aligned and anti-aligned librations, respectively.

a (au)	k_6 interval (arcsec yr^{-1})		
	All librations	Aligned	Anti-aligned
2.00	$[-1, +1]$	$[-1, 0]$	$+1$
2.24	$[-2, +2]$	$[-2, 0]$	$[+1, +2]$
2.39	$[-3, +3]$	$[-3, -2]$	$[0, +3]$
2.48	$[-4, +3]$	$[-4, -2]$	$[-1, +3]$
2.56	$[-5, +3]$	$[-5, -3]$	$[-3, +3]$
2.66	$[-6, +3]$	$[-6, -4]$	$[-5, +3]$
2.76	$[-6, +3]$	$[-6, -5]$	$[-6, +3]$
2.86	$[-6, +3]$	-6	$[-6, +3]$
2.96	$[-6, +3]$		$[-6, +3]$
3.05	$[-6, +3]$		$[-6, +3]$
3.25	$[-6, +2]$		$[-6, +3]$

asteroids located at low inclinations ($I < 20°$) and/or values of $a < 2.5$ au. The dynamical behaviour of asteroids at high inclinations ($I > 20°$), and/or values of $a > 2.5$ au, is represented by equation (3). Using these equations, it is possible to localize the resonant region where the libration states occur, and to identify asteroids that may be stuck there.

Figs 1 and 2 show the level curves in the plane (σ_6, e) of the Hamiltonian equations (2) and (3), respectively. These curves are plotted for fixed values of the parameter $k_6 = b - g_6$ and the inclination I. Values in the range $-6 \le k_6 \le +6$ arcsec yr^{-1} were selected to get the closest neighbourhood of the ν_6 secular resonance. We varied the semi-major axis a between 2.0 and 3.34 au to cover the classical main asteroid belt. At each region of the belt (inner: $2.0 < a < 2.5$ au; middle or central: $2.5 < a < 2.82$ au; and outer: $2.82 < a < 3.3$ au), we consider four different fixed values of a. These values of a were chosen only to provide an example of how the libration state depends on the semi-major axis.

In Fig. 1, we find aligned librations only for values of eccentricity $e > 0.5$ in the inner belt (panels A and B). The anti-aligned librations are present throughout most of the main belt, with decreasing eccentricities for larger semi-major axes. In the outer belt, we identify orbits circulating counterclockwise (panels K and L). In Fig. 2, the extrema of the main belt show orbits circulating counterclockwise (panels A, B) or clockwise (panels K, L), respectively. Aligned librations appear at high e in the inner belt, but reach smaller eccentricities at the central and outer belt. On the other hand, anti-aligned librations appear at small eccentricities in the inner and central belt, and disappear in the outer belt. It is worth noting that the portraits shown in Figs 1 and 2 are specific for the indicated values of k_6, and have been chosen only as examples to give a global view of the resonant behaviour. The chosen values encompass the extrema of resonant motion, from solutions lying very close to the resonance centre (~ 0.3 arcsec yr^{-1}) to solutions lying far from the resonance centre (~ 3 arcsec yr^{-1}).
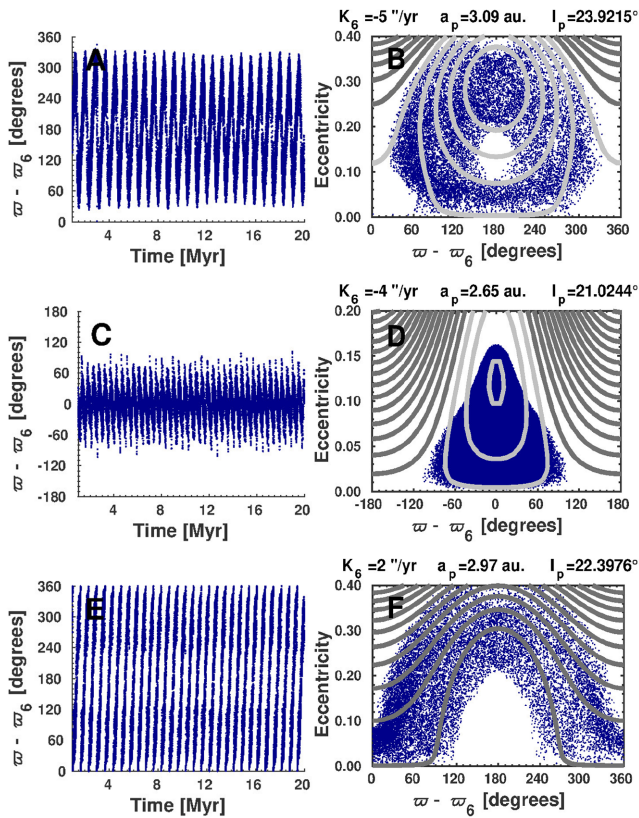
Figure 3. Temporal evolution of the resonant argument $\sigma_6 = \varpi - \varpi_6$ of asteroids (322770) 2001 FD145 (panel A), (337335) 2001 EQ18 (panel C), and (154204) 2002 HL8 (panel E), exemplifying the three possible dynamical states related to the ν_6 resonance: anti-aligned libration (around 180°), aligned libration (around 0°), and circulation, respectively. Panels B, D, and F show the evolution in the plane (σ_6, e) (blue dots), overlapped to the level curves of the analytical model for the corresponding value of k_6 (see text). Light grey levels identify the libration domains, while dark grey levels identify the circulation domain (note the different horizontal scale limits between panels B and D). The values of a_p and I_p are the synthetic proper elements of each asteroid, from AstDyS.

Other values of k_6 will produce different portraits. In Table 1, we present a summary of the ranges in k_6 leading to resonant behaviour in terms of the semi-major axis, following our analysis of the Hamiltonian phase space (equations 2 and 3) throughout the main belt.

Our study of the analytical model allows us to conclude that the width of the libration region of main-belt asteroids in the ν_6 resonance is, in general, $-6 \leq k_6 \leq +3\,\mathrm{arcsec\,yr^{-1}}$. This analytical model, however, provides a limited contribution to address the actual dynamical evolution of resonant asteroids. In particular, the model is not accurate for large eccentricities. Nevertheless, we can use the above results to roughly estimate the boundaries of the aligned and anti-aligned libration regions, and apply this as a starting point to try to identify real asteroids trapped in these resonant states.

In order to better estimate the libration domain of the ν_6 resonance, we define a libration parameter, k_{Lib}, using the divisor $k_{\mathrm{Lib}} = g_p - g_6$, where g_p is the proper frequency of the asteroid perihelion and g_6 is that of Saturn. Both frequencies, g_p and g_6, may be computed either from an analytical theory (e.g. Brouwer & van Woerkom 1950; Milani & Knežević 1990) or from a synthetic numerical theory (e.g. Nobili, Milani & Carpino 1989; Knežević & Milani 2003), and each theory may give different values of k_{Lib},

even for the same asteroid. In our case, the value of k_{Lib} is only taken as a reference to select resonant candidates, and we assume that resonant motion may be constrained by the condition $-3.5 \leq k_{\mathrm{Lib}} \leq +3.0\,\mathrm{arcsec\,yr^{-1}}$. This constraint is based on our previous knowledge of the libration domain provided by the parameter k_6 of the Yoshikawa (1987) model (cf. Table 1). It is worth noting, however, that k_{Lib} is equivalent to but not the same as k_6, because they are obtained from essentially different approaches. Nevertheless, using k_6 as a proxy, we expect that our assumption for k_{Lib} encompasses a wide region where asteroids could be in libration states. We recall that other authors assume narrower values, like Froeschlé et al. (1995) ($0.35 \leq k_{\mathrm{Lib}} \leq 1.5\,\mathrm{arcsec\,yr^{-1}}$) or Carruba (2009) ($-2.55 \leq k_{\mathrm{Lib}} \leq 2.55\,\mathrm{arcsec\,yr^{-1}}$).

Here we use two different sets of proper elements a_p, e_p, $\sin I_p$, and frequencies g_p to compute the values of k_{Lib}. The first set is given by the synthetic theory of Knežević & Milani (2003), and it is listed in the AstDys catalogue of synthetic proper elements (version of 2017 April 16; available at hamilton.dm.unipi.it/astdys/). The main advantage of this catalogue is that it provides the values of the proper frequencies for a very large set of asteroids, with especially accurate values for high-eccentricity and high-inclination orbits (which is, in general, the main limitation of the analytical theories). The second set of proper elements/frequencies is computed by ourselves for a limited number of asteroids, from a digital filtering of the series $e\cos\varpi$, $e\sin\varpi$, as explained in the next section.

3 DYNAMICS OF ASTEROIDS INTERACTING WITH THE ν_6 RESONANCE

Taking into account the resonant domain defined in the previous section, we identify 4 137 asteroids from the AstDys catalogue that might interact with the ν_6 resonance in libration states according to their values of k_{Lib}. This candidate population spans a range in $2.0107 \leq a_p \leq 3.276\,\mathrm{au}$, $0.010 \leq e_p \leq 0.434$, $0.435° \leq I_p \leq 33.322°$, and absolute magnitude $H < 20$. In principle, only some of these asteroids are expected to stay in pure libration states, while most of them are expected to interact with the ν_6 resonance partially, by alternating between libration and circulation states.

In order to find the pure librators, we perform a numerical simulation of the orbital evolution of these 4 137 candidates using the symplectic N-body integrator SWIFT_MVS (Levison & Duncan 1994), including the modifications by Brož (1999). Our model takes into account the direct perturbation of the planets from Venus to Neptune, and the indirect perturbation of Mercury through the corresponding barycentric correction to the position and velocity of the Sun. The simulations span 20 Myr, with a time-step of 2 days. Such a time-span is long enough to detect the long-term effects of secular resonances (Carruba & Machuca 2011b), and to identify the orbits that are presently locked inside the ν_6 resonance. Examples of the behaviours identified by this procedure are shown in Fig. 3 for asteroids (322770) 2001 FD145 (anti-aligned libration), (337335) 2001 EQ18 (aligned libration), and (154204) 2002 HL8 (circulation). In the right-hand panels of Fig. 3, we overlap the dynamical evolution of the orbits in the (σ_6, e) phase space to the Hamiltonian level curves of the analytical model (Section 2).

We found that 803 asteroids display pure librations (aligned and anti-aligned) around the equilibria of the ν_6 resonance. Most of these asteroids have small proper eccentricities, in general less than 0.15. We also found that 545 asteroids were removed from the main belt before 20 Myr by planetary close encounters. Of these, 413 displayed temporary librations (either aligned, anti-aligned, or both) alternated with circulations, before being ejected. We do not
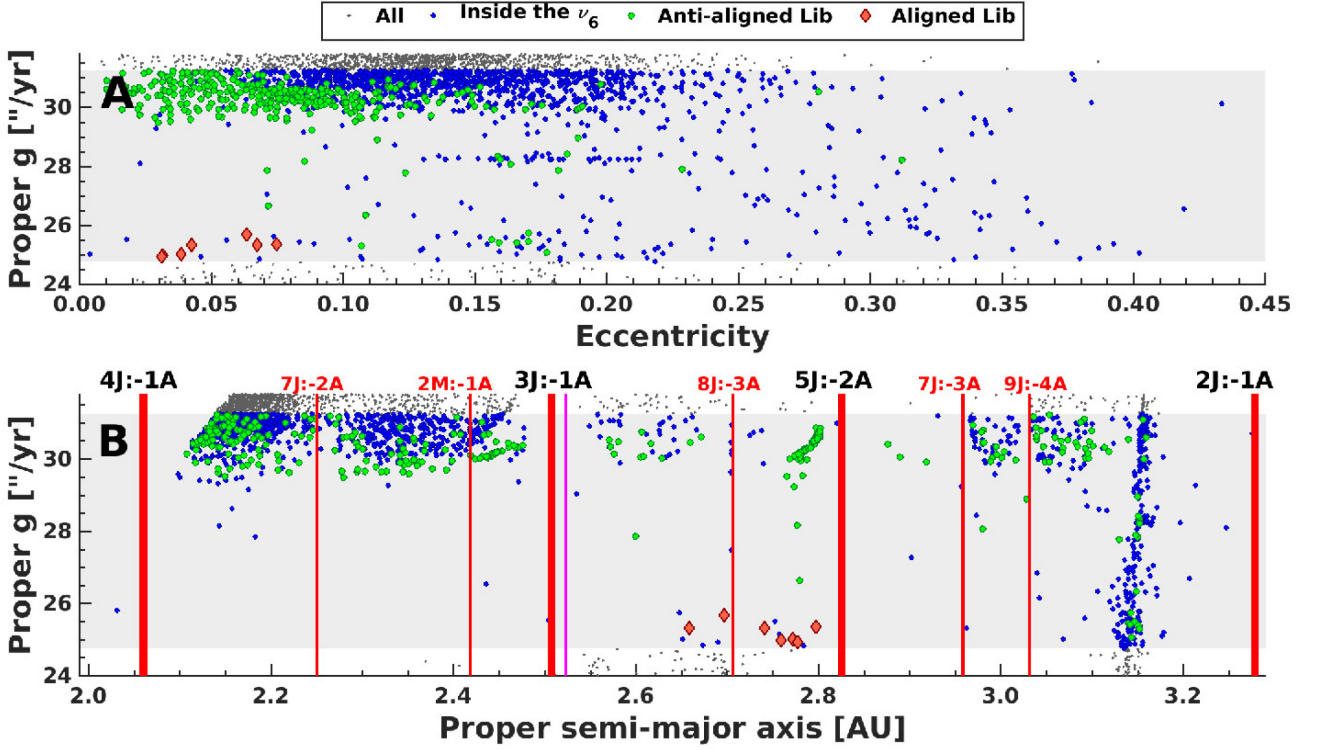
Figure 4. Distribution of asteroids around the ν_6 secular resonance, projected onto the planes (g_p, e_p) (panel A) and (g_p, a_p) (panel B). The proper elements and frequency come from AstDyS (Knežević & Milani 2003). The grey area represents the resonance domain. Dark grey dots are main-belt asteroids that are unlikely to be affected by the resonance. Green circles represent anti-aligned librators, red diamonds represent aligned librators, and blue circles either are circulators or alternate between libration and circulation. The classification is based on a 20 Myr numerical simulation of the orbital evolution. Vertical red lines in panel B give the approximate location of the main mean motion resonances with Jupiter and Mars. The vertical alignment of orbits observed at about 3.1 au in panel B is related to forced oscillations induced by the nearby 2:1 mean motion resonance with Jupiter.
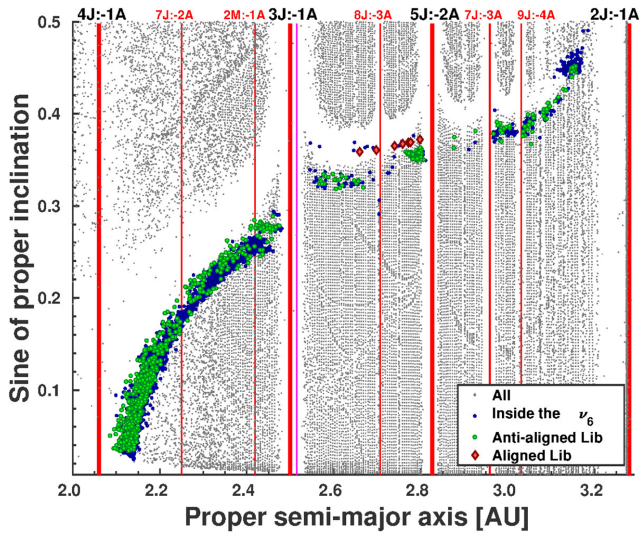

Figure 5. Distribution of the 4 137 asteroids (coloured symbols) that interact with the ν_6 resonance. The colour code is the same in Fig. 4. Dark grey dots represent proper elements of an initially uniform grid of test orbits (see text for explanation). Vertical red lines indicate the location of the main mean motion resonances.
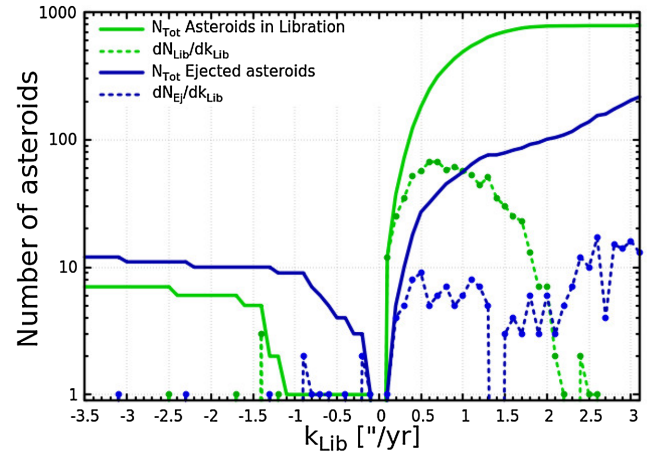
Figure 6. Distributions in terms of k_{Lib} of the number of asteroids that are in pure libration states, both aligned and anti-aligned, over 20 Myr of evolution (803 asteroids, in full green line), and those asteroids that escape due to planetary encounters over the same time-span (545 asteroids, in full blue line). Dashed lines with dots are the differential distributions at bins of 0.1 arcsec yr^{-1}. Full lines are the cumulative distributions.

find any preference for the ejection to happen when the orbit was librating or circulating.

In Fig. 4, we show the distribution of the real asteroids (with symbols) that lie close to or inside the ν_6 secular resonance, projected onto the planes (e_p, g_p) (panel A) and (a_p, g_p) (panel B). The assumed domain of the resonance $(g_6 \pm k_{Lib})$ is indicated by the grey area; the 4 137 candidates analysed in this study lie within this region. Green circles represent the orbits in pure anti-aligned libration (796 asteroids), while red diamonds are those in pure aligned libration (7 asteroids). Blue circles (3 334 asteroids) display either pure circulation or alternate between libration and circulation. Strong depletion is observed at the locations of the main mean motion resonances with Jupiter (vertical lines in panel B), as expected. While the anti-aligned librators appear to be spread throughout the whole asteroid belt (with a concentration at the inner belt), with values of k_{Lib} mostly positive, the aligned librators appear restricted to the central belt, with negative values of k_{Lib}, in good agreement with the predictions of the analytical model (see Section 3.1).

Interestingly, both populations of pure librators (aligned and anti-aligned) are found close to the edges of the resonant domain, giving the impression that libration amplitudes of σ_6 tend to be large. The central part of the resonant domain, close to the equilibria $(g_p \simeq g_6)$, is empty. This seems to be an artefact of using the Ast-Dys synthetic proper elements, which are not suitable to describe the distribution of asteroids locked in librating states (e.g. Milani et al. 2017). Actually, 80.7 per cent of the 4 137 asteroids in our sample show errors in the proper eccentricity $\sigma(e) > 0.01$, while 48,2 per cent show $\sigma(e) > 0.02$, and 25 per cent show $\sigma(e) > 0.03$.[1] The errors in a_p and $\sin I_p$, on the other hand, are almost negligible [0.01 per cent with $\sigma(a) > 0.01$, and 0.16 per cent with $\sigma(\sin I) > 0.01$]. Such significant errors in e_p are produced by the proximity of the orbits to the strong ν_6 secular resonance. As pointed out by Milani et al. (2017), this happens because the standard computation of the synthetic proper elements applied to resonant orbits is affected by the presence of resonant modes that generate large oscillations of the resulting proper elements. Therefore, to overcome this limitation, it is necessary to compute proper elements and frequencies specifically tailored for the ν_6 resonance.

Here we recompute the synthetic proper elements/frequencies for the 803 asteroids in librating states following the approach described in Carruba (2010). This approach applies the frequency-modified Fourier transform method of Sidlichovský & Nervorný (1996) to filter the series $e \cos \varpi$, $e \sin \varpi$. We consider a time-span of this series of 2 Myr, and apply a two-stage filter to obtain values of the proper element/frequency every 150 kyr. Then we compute the average proper element/frequency and their corresponding σ dispersions over the whole time-span. These proper elements and frequencies differ from those provided by the AstDys catalogue, and they display much smaller σ dispersions. Thus, they are expected to be more suitable to describe the distribution of asteroids close to the ν_6 resonance.

In Fig. 5, we plot the distribution of 4 137 asteroids that interact with the ν_6 resonance projected onto the $(a_p, \sin I_p)$ plane. The distribution is overlapped by a dynamical map of the whole main belt (dark grey dots) obtained by computing synthetic proper elements for a grid of orbits, as explained above. The grid is constituted of $220 \times 350 = 77\,000$ test particles with osculating initial conditions

---

[1]The error $\sigma(e)$ is given in the AstDys catalogue, and it is a measure of the stability of the computed proper element, i.e. how much the proper element is expected to change over a long time-span.
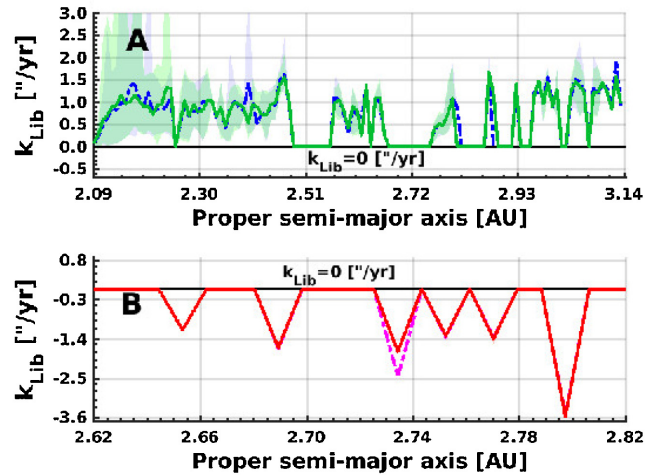
Figure 7. Distribution of values of k_{Lib} with respect to a_p for the anti-aligned (panel A) and the aligned (panel B) pure librators, respectively. The distributions are binned every 0.005 au. Full lines represent the mean value at each bin; the green area in panel A spans the maximum and minimum values at each bin. No similar area is plotted in panel B since the distribution of aligned librators is limited to six asteroids. The dashed blue and magenta lines give the distributions in terms of the present proper frequency, while the full green and red lines give the distribution in terms of the frequency computed after 20 Myr of evolution.

distributed uniformly in the (a, I) plane, with a spacing of 0.005 au and $0.2°$. The initial values of the remaining osculating orbital elements e, ϖ, Ω (longitude of node), and λ (mean longitude) of each test particle of the grid have been arbitrarily fixed to those of asteroid (410) Chloris, an asteroid located in the central main belt. Therefore, the dynamical map is expected to represent a slice of the proper elements space at constant $e_p \simeq 0.26$. Both the grid of initial conditions and the 4 137 asteroids are evolved using the symplectic integrator SWIFT_MVS over 20 Myr, and accounting for the gravitational perturbations of all the planets as previously described. It is worth noting that the synthetic proper elements for the real asteroids and the grid test particles are calculated from this evolution during the last 2 Myr, i.e. between 18 and 20 Myr.

Forty-five per cent of the initial grid is depleted during the simulation, so the dynamical map in Fig. 5 gives the distribution of the surviving 42 300 orbits. As expected, the ν_6 resonance opens a wide gap in the grid all across the main belt, providing a barrier that shapes the upper boundary in the inclination of the asteroid belt. The large depletion of test particles observed around ~2 au is related to the overlap of the ν_6 resonance with other resonances, in particular the ν_{16}. We note that the aligned librators (red diamonds) are located at higher inclinations than the anti-aligned librators (green circles) in the same region of the main belt. This is related to the fact that the former have smaller values of g_p ($k_{Lib} < 0$) than the latter (compare to Fig. 4).

Once we have identified the 803 asteroids currently in pure libration states (both aligned and anti-aligned), and we have recalculated their proper elements and frequencies, we may use them to reassess the range of k_{Lib} that characterizes the resonant motion. In Fig. 6, we show the differential (dashed green line) and cumulative (full green line) distributions of the number of librating asteroids as a function of k_{Lib}. In this case, k_{Lib} was calculated using the 'current' proper frequency, i.e. the proper frequency computed over the first 2 Myr of evolution. The figure also displays the differential and cumulative distributions (in full blue line) of the 545 asteroids that

Table 2. List of asteroids evolving in either pure aligned libration or alternating between aligned libration and circulation. The second column gives the absolute magnitude; the third to sixth columns give the values of the synthetic proper elements and perihelion frequency; the last two columns are the backward and forward lifetimes of the orbits, indicating when applicable whether the orbit is scattered to the inner (I) or to the outer (O) Solar System. A (∗) symbol identifies the orbits that remain in pure aligned libration over 400 Myr of evolution.

Asteroid number	H	a_p	e_p	$\sin I_p$	g_p	T_{surv}^-	T_{surv}^+
		(au)			(arcsec yr^{-1})	(Myr)	(Myr)
Currently in pure libration							
337335 (∗)	15.26	2.6583	0.04246	0.3587	25.3124	200.0	200.0
143199	15.05	2.6971	0.06351	0.3604	25.6695	200.0	200.0
295883	15.45	2.7413	0.06737	0.3650	25.3128	200.0	200.0
73415 (∗)	14.76	2.7591	0.03151	0.3671	24.9691	200.0	200.0
322878 (∗)	15.76	2.7718	0.03859	0.3680	25.0071	200.0	200.0
371246 (∗)	15.68	2.7771	0.03122	0.3688	24.9152	200.0	200.0
203236	14.63	2.7978	0.07478	0.3718	25.3434	200.0	200.0
Currently alternating							
397488	16.84	2.5453	0.03481	0.3689	24.8544	14.1 (I)	27.6 (I)
248158	15.61	2.6732	0.06833	0.3628	24.8347	163.1	200.0
401320	16.74	2.6765	0.09075	0.3638	24.8219	129.5	200.0
354463	15.91	2.6901	0.04604	0.3629	24.9176	200.0	200.0
364329	16.84	2.6948	0.07527	0.3624	25.2392	200.0	200.0
314787	16.11	2.7511	0.06212	0.3658	25.2298	200.0	200.0
257972	15.07	3.1245	0.21953	0.4399	25.2417	18.3 (O)	6.3 (O)
179554	14.70	3.1282	0.23968	0.4437	25.1906	13.6	114.1
88064	13.43	3.1289	0.28837	0.4496	25.0522	12.9 (O)	80.2
246505	14.52	3.1362	0.29986	0.4529	25.7276	115.7 (O)	8.8 (O)
320989	15.20	3.1378	0.32547	0.4572	25.5468	131.1 (O)	9.8 (O)
282444	14.73	3.1384	0.19053	0.4474	24.9942	54.4	52.7
220835	14.73	3.1391	0.20395	0.4494	24.9588	19.6 (O)	16.5 (O)
121759	13.91	3.1403	0.17451	0.4463	25.6889	200.0	49.1
56932	13.51	3.1427	0.16097	0.4473	26.1453	200.0	15.7
313169	14.53	3.1464	0.29678	0.4585	26.7213	17.4 (O)	18.0 (O)
344837	15.08	3.1522	0.21230	0.4527	28.2298	200.0	67.5 (O)
267506	14.79	3.1522	0.27848	0.4504	31.1599	8.4 (O)	21.8 (O)
406770	15.28	3.1530	0.26629	0.4525	30.4131	56.3	55.1 (O)
165949	14.51	3.1533	0.35400	0.4742	25.1702	56.2 (O)	16.6 (O)
402513	15.07	3.1537	0.29342	0.4547	30.6264	200.0	102.4 (I)

were removed from the main belt by planetary close encounters. We note that the distribution of anti-aligned resonant orbits shows values of $k_{Lib} > 0$, as expected, with a maximum at 0.6 arcsec yr^{-1}. The corresponding cumulative distribution saturates for values of $k_{Lib} > 2.5$ arcsec yr^{-1}. On the other hand, the distribution of aligned resonant orbits shows values of $k_{Lib} < 0$, and the cumulative distribution saturates for $k_{Lib} < -2.5$ arcsec yr^{-1}. These saturation limits better define the criterion for resonant motion to arise. Concerning the escaping orbits, we note an increasing number of them for $k_{Lib} > 2$ arcsec yr^{-1}, which is related to the fact that the sample of 4 137 candidates is concentrated at positive values of k_{Lib}, especially in the inner belt.

Fig. 7 shows the distribution of values of k_{Lib} in terms of the proper semi-major axis for the 803 asteroids in pure libration states. The distribution of the population is given in terms of the 'current' proper frequencies, i.e. the proper frequency computed over the first 2 Myr of evolution (dashed blue and magenta lines for anti-aligned and aligned libration, respectively), and also in terms of the proper frequencies computed over the last 2 Myr of evolution (full green and red lines for anti-aligned and aligned libration, respectively). These latter correspond to the proper elements shown in Fig. 5. The full and dashed lines represent the mean value of k_{Lib} at each

bin of 0.005 au. For the anti-aligned librators (panel A), the green shaded area encompasses the maximum and minimum values of k_{Lib} at each bin. No significant differences are appreciated between the current frequency and the frequency after 20 Myr. Fig. 7 contrasts with the distribution shown in Fig. 4, confirming that the frequencies we compute seem to be much more suitable to describe the secular resonant motion than those of AstDys, as previously mentioned.

3.1 The aligned librators

Asteroids in anti-aligned libration of the ν_6 resonance have been previously identified by other authors, but asteroids in aligned libration are actually a new finding. The sparse number of such bodies, and in particular the lack of them in the inner belt, seems to be related to the significant depletion observed in the regions of the main belt where they are likely to be found. The analytical model of Yoshikawa (1987) shows that aligned librators must always have small eccentricities, and should be found for values of $-3.0 \leq k_6 \leq 1.0$ arcsec yr^{-1} in the inner belt and values of $k_6 \leq -2.0$ arcsec yr^{-1} in the central and outer belt.
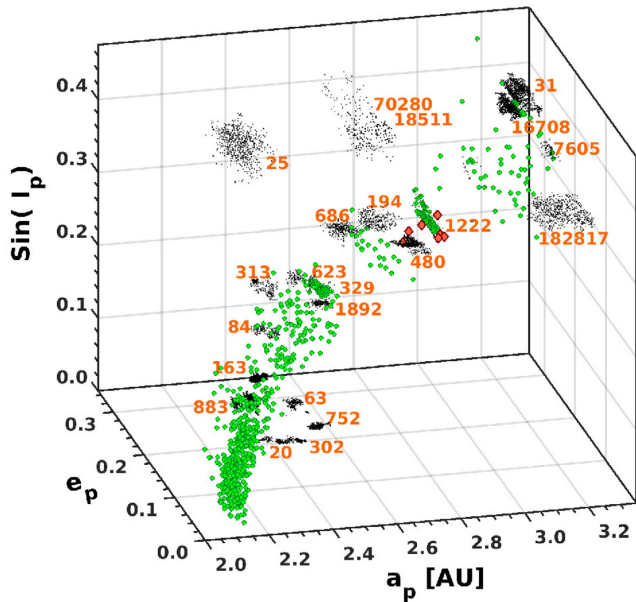
Figure 8. Distribution in the 3D space of proper elements of the 25 asteroid families (clusters of black dots) considered in this study. The population of the ν_6 pure librators is also shown (green circles and red diamonds for anti-aligned and aligned, respectively). To plot the families, we take into account only asteroids with absolute magnitude $H < 16$. Numbers correspond to the numbers of the asteroids that give the name to each family. The pure librators are displayed in terms of the proper elements computed in Section 3 (Fig. 5). The families are displayed in terms of the AstDys proper elements (Knežević & Milani 2003).

In this study, we identify for the first time 7 asteroids currently in aligned libration, all in the central main belt with values of k_{Lib} ranging from -3.3 to -1.2 arcsec yr^{-1}. Asteroid (337335) 2001 EQ18, whose evolution is shown in Fig. 3, is one of them. It is worth noting that this classification is based on the orbital behaviour over a 20 Myr time-span only. Besides, we identified 21 other asteroids in the central and outer main belt that alternate between aligned libration and circulation over 20 Myr. These asteroids are reported in Table 2.

We analysed the long-term orbital stability of this population of 28 asteroids by extending our numerical simulations to 200 Myr into the future and 200 Myr into the past. The initial conditions for the backwards simulations were set up by changing the sign of the Cartesian velocity components, following the procedure described in Carruba, Nesvorný & Vokrouhlický (2016). In order to track the orbits backwards with enough precision, we set the time-step of these simulations to 1 day. The results show that only 4 of the 7 asteroids classified as pure librators remained in stable orbits with the resonant argument σ_6 always librating around $0°$ for the whole 400 Myr time-span. These are indicated in Table 2 by the symbol (∗). The other 3 pure librators are affected by the nearby 8:3 mean motion resonance with Jupiter, and start to alternate between libration and circulation. The asteroids that survive in stable orbits for the whole time-span, with the resonance argument alternating between libration (aligned and/or anti-aligned) and circulation, are observed in the region of semi-major axis $2.69 < a_{\mathrm{p}} < 2.75$ au and eccentricity less than 0.08.

The remaining asteroids, i.e. those that do not survive over the 400 Myr time-span, represent more than half of the asteroids that alternate between libration and circulation of the resonant argument,

and are scattered into the outer belt (with semi-major axis $3.12 < a_{\mathrm{p}} < 3.154$). They are removed by planetary close encounters, in most cases with Jupiter. The lifetimes of these orbits are reported in the last two columns of Table 2.

4 ASTEROID FAMILIES INTERACTING WITH THE ν_6 RESONANCE

Asteroid families are groups of asteroids that have a common origin from the collisional fragmentation of a larger parent body. Identifying an asteroid family that may interact with a secular resonance is relevant, since the dynamical lifetimes of the resonant family members may help to constrain the age of the family.

Here, we consider a list of 195 known asteroid families and clumps in the main asteroid belt that have been reported by different authors (Mothe-Diniz, Roig & Carvano 2005; Gil-Hutton 2006; Carruba & Machuca 2011b; Machuca & Carruba 2012; Carruba et al. 2014; Milani et al. 2014; Nesvorný, Brož & Carruba 2015; Spoto, Milani & Knežević 2015; Milani et al. 2016), and from this list, we select 25 families that are located in the neighbourhood of the ν_6 resonance domain. The distribution of these families is shown in Fig. 8 (black dots), together with the population of aligned (red diamonds) and anti-aligned (green circles) librators. Among the selected families, there are the families of Tina and Euphrosyne, which have been previously identified as interacting with the ν_6 resonance. Besides, we identify four other families that also appear to partially interact with this resonance: Lucienne, Svea, Cindygraber, and 1995 SP1. We will focus, hereafter, on the first two.

Since an asteroid family forms a cluster in the space of proper elements, a usual method to detect families is the hierarchical clustering method (Zappalà et al. 1990). This consists in defining a distance metric in terms of proper elements, $d(a_{\mathrm{p}}, e_{\mathrm{p}}, \sin I_{\mathrm{p}})$, and to group together pairs of asteroids for which the mutual distance is less than a given cut-off value. The form of the metric is related to the shape of the ejection velocity field during the formation of the family, and the cut-off distance is the expected maximum ejection velocity, v_{cut}. Therefore, the larger the v_{cut}, the larger the number of asteroids that become members of a given family.[2]

Fig. 9 shows the number of members of the Lucienne (panel A) and Svea (panel B) families as a function of the cut-off velocity. The blue line is the cumulative number, while the cyan line is the differential distribution. In order to determine the minimum and maximum possible number of family members, we take into account the peaks in the differential distribution. For example, the family of Lucienne starts with 37 members at $v_{\mathrm{cut}} = 37$ m s^{-1} and reaches a maximum of 254 members at $v_{\mathrm{cut}} = 152$ m s^{-1}. For larger cut-off values, the family slowly expands including peripheral objects that might not be true members of the family: the so-called halo of the family.

In Fig. 10, we show the distribution of the Lucienne (circles) and Svea (diamonds) family members projected onto the $(a_{\mathrm{p}}, \sin I_{\mathrm{p}})$ plane (panel A) and the $(g_{\mathrm{p}}, \sin I_{\mathrm{p}})$ plane (panel B). Both families are located in the inner main belt, in a narrow region between the 2:1 mean motion resonance with Mars and the 3:1 mean motion

---

[2]We use the standard metric

$$d = na_{\mathrm{p}}\sqrt{\frac{5}{4}\left(\frac{\delta a_{\mathrm{p}}}{a_{\mathrm{p}}}\right)^2 + 2\left(\delta e_{\mathrm{p}}\right)^2 + 2\left(\delta \sin I_{\mathrm{p}}\right)^2} \quad (4)$$

where n is the orbital mean motion (so d has units of m s^{-1}), and $(\delta a_{\mathrm{p}}, \delta e_{\mathrm{p}}, \delta \sin I_{\mathrm{p}})$ are the mutual separations.
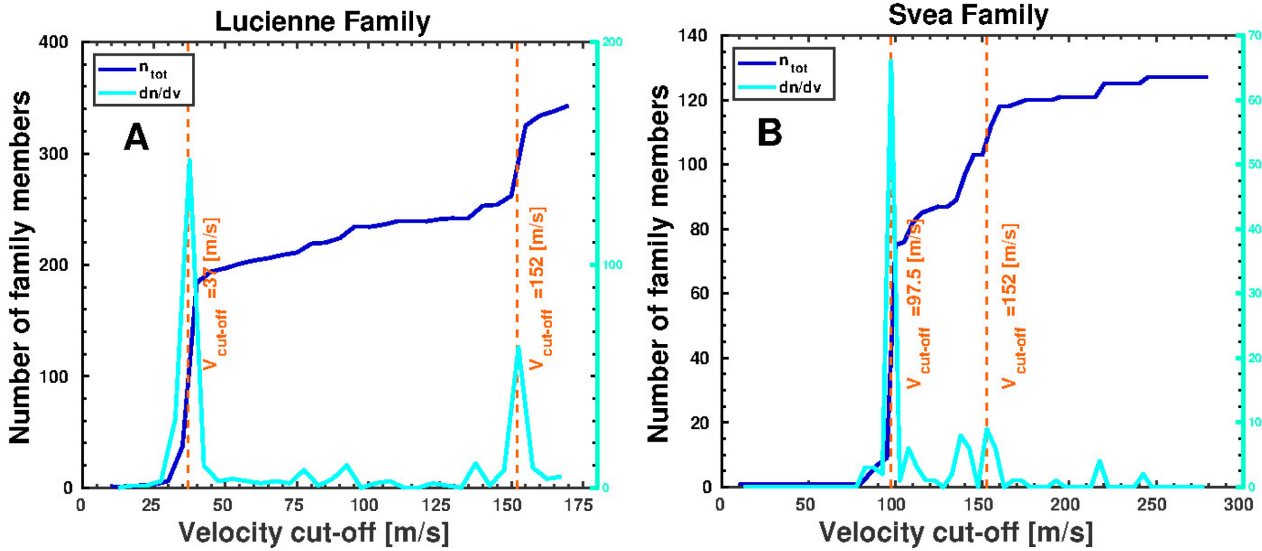
Figure 9. The number of asteroid members of the Lucienne (panel A) and Svea (panel B) families as a function of the cut-off velocity. The blue and cyan lines are the cumulative and differential distributions, respectively. The vertical dashed lines indicate the cut-off limits to define the minimum and maximum number of members in each family.
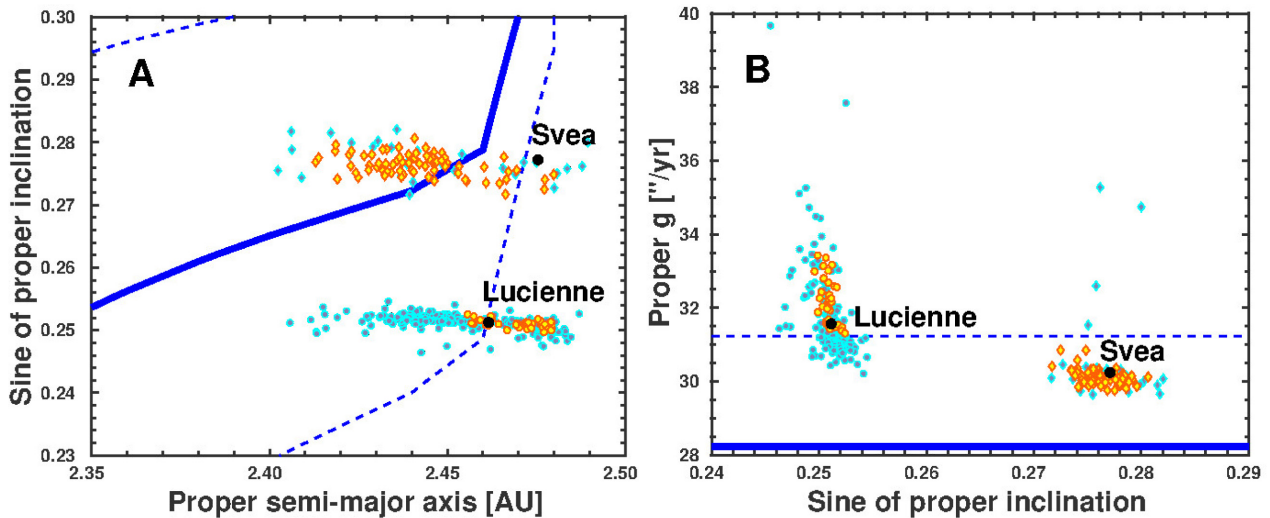

Figure 10. Distribution of the members of the Lucienne (circles) and Svea (diamonds) families in the space of proper elements and *g* frequency (from the AstDys catalogue). The minimum number and maximum number of members are identified by the orange and cyan colours, respectively. The blue lines determine the centre (full) and approximate borders (dashed) of the ν_6 resonance.

resonance with Jupiter. The orange and cyan colours identify the family members for the considered minimum and maximum values of v_{cut}, respectively. The full blue line corresponds to the locus of the ν_6 resonance, computed using the analytical model of Milani & Knežević (1994) for a fixed eccentricity of 0.1 [i.e. compatible with the proper eccentricities of asteroids (1892) Lucienne and (329) Svea]. The blue dotted lines approximately encompass the resonant domain.

As we can see, the Svea family is strongly influenced by the ν_6 resonance. For the maximum cut-off, we find 56 members (54 per cent) of this family evolving in anti-aligned libration. For the Lucienne family, on the other hand, we find only one member evolving in an

anti-aligned libration state. Interestingly, neither (1892) Lucienne nor (329) Svea is in a resonant state, having their critical arguments always circulating.

The same procedure described above has been applied to the other families and clumps presented in Fig. 8.[3] We recover the results by Carruba & Morbidelli (2011a) for the Tina family; we identified 86 family members (90 per cent) in anti-aligned libration. We also recover the results for the Euphrosyne family (Carruba

[3]Baptistina, Chimaera, Datura, Flora, Klio, Levin, Lucascavin, Massalia, Matterania, Phocaea, Sulamitis, Vesta, Emilkovalski, Gersuind, Hansa, Tina, Watsonia, 2000 DL37 Cindygraber, Euphrosyne, 1995 SP1, 2000 DQ94.

Table 3. Asteroid families and clumps that interact with the ν_6 secular resonance. The second and third columns give the minimum and maximum cut-off values considered to define the family, the fourth column gives the maximum number of members, and the fifth column indicates the number of members in anti-aligned libration.

Family name	Min. v_{cut} (m s^{-1})	Max. v_{cut} (m s^{-1})	Members	Librators
(1892) Lucienne	37	150	254	1
(329) Svea	97.5	150	103	56
(1222) Tina	200	260	96	86
(31) Euphrosyne	45	95	3408	20
(7605) Cindygraber	95	135	93	2
(16708) 1995 SP1	32.5	45	331	4

et al. 2014), with 20 members in anti-aligned libration. Finally, we identify in the outer main belt two clumps with few members also in anti-aligned libration. Our results are summarized in Table 3.

As stated in Section 3, the drawback of using the synthetic proper elements provided by AstDys is that they are not expected to be accurate enough for asteroids evolving inside the ν_6 resonance. Therefore, in the case of asteroids in librating states, it would be necessary to substitute the standard e_p by a suitable resonant proper element Δe_p (e.g. Milani et al. 2017). This resonant proper eccentricity can be roughly computed, for example, as the amplitude $|e_{max} - e_{min}|$ between the minimum and maximum values of the filtered series of $e \cos \sigma_6$, $e \sin \sigma_6$. Nevertheless, this procedure would not help to improve the analysis of the families, because not all the members are purely resonant, and the proper elements e_p and Δe_p are not comparable to each other. Only in the case of the Tina family, which has most of its members inside the ν_6 resonance, would this procedure be worth applying.

5 CONCLUSIONS

We identify and study the dynamical evolution of asteroids affected by the ν_6 secular resonance in the main belt, with particular emphasis on those bodies that exhibit states of pure libration. Our results can be summarized as follows:

(i) From a simulation of the dynamical evolution over 20 Myr, we identify a population of 803 asteroids that are trapped in either aligned libration (resonant argument $\varpi - \varpi_6$ oscillating around $0°$) or anti-aligned libration (resonant argument oscillating around $180°$).

(ii) The population of asteroids in aligned libration is constituted by only seven objects, all located in the central main belt. This is the first time that such a kind of aligned librators have been detected. Our numerical simulations of their orbits over ± 200 Myr show that only 4 of them remain in stable aligned libration ($e \sim 0.1$) over the whole time-span, while the other three are also stable, but at some point they begin to alternate their resonant argument moving between phases of libration and circulation, with $e < 0.3$.

(iii) The population of asteroids that are presently alternating between aligned libration and circulation is constituted by 21 bodies in the middle and outer main belt. More than half of these asteroids are unstable over a ± 200 Myr time-span, being scattered to the outer belt and removed by planetary close encounters.

(iv) The largest depletion of the ν_6 resonance occurs in the regions where the analytical model of Yoshikawa (1987) predicts that

asteroids should be found in aligned libration states. This would be the reason why the population of such bodies is presently too small.

(v) We identified two new asteroid families, Svea and Lucienne, both in the inner main belt, and two new clumps, Cyndygraber and 1995 SP1, in the outer main belt, which have members that interact with the ν_6 resonance in anti-aligned libration states. In particular, the Svea family has the second largest population of resonant members, following the family of Tina (Carruba & Morbidelli 2011a).

Our results indicate that the ν_6 secular resonance is a very effective mechanism of depletion throughout the main asteroid belt. The resonance affects the presently known asteroid families very little, with a few exceptions, basically because any large family fully formed in the resonant domain would have been quickly depleted/dispersed and is no longer there to be detected. The only exceptions are the small families of Svea, Tina, and a group of asteroids in aligned libration that are inside the resonance but can be stable for hundreds of Myr. We conclude that these asteroids and families are particularly stable because they do not interact with other dynamical mechanisms, such as mean motion and other linear and non-linear secular resonances. A study of their stability over longer time-scales would require taking into account the Yarkovsky and YORP effects, but that is beyond the scope of this work. In any case, such studies would help to set tight constraints to the ages of these small families.

REFERENCES

Brouwer D., van Woerkom A. J. J., 1950, Astron. Papers Amer. Eph. and Naut. Alm., 13, 81
Brož M., 1999, Master's thesis. Charles University, Prague
Carruba V., 2009, MNRAS, 395, 358
Carruba V., 2010, MNRAS, 408, 580
Carruba V., Morbidelli A., 2011a, MNRAS, 412, 2040
Carruba V., Machuca J., 2011b, MNRAS, 418, 1102
Carruba V., Aljbaae S., Souami D., 2014, ApJ, 792, 46
Carruba V., Nesvorný D., Vokrouhlický D., 2016, AJ, 151, 164
Charlier C. V. L., 1902, Die Mechanik des Himmels. Verlag Von Veit & Comp., Leipzig, 410
Froeschlé C., Scholl H., 1993, Cel. Mech. Dyn. Astron., 56, 163
Froeschlé C., Hahn G., Gonczi R., Morbidelli A., Farinella P., 1995, Icarus, 117, 45
Gil-Hutton R., 2006, Icarus, 183, 93
Hagihara Y., 1928, Proc. of the Physico-Mathematical, Soc. of Japan, 3rd series, Vol 10., 127
Knežević Z., Milani A., 2003, A&A, 403, 1165
Knežević Z., Milani A., Farinella P., Froeschlé C., Froeschlé C., 1991, Icarus, 93, 316

Levison H. F., Duncan M. J., 1994, Icarus, 108, 18

Machuca J. F., Carruba V., 2012, MNRAS, 420, 1779

Milani A., Knežević Z., 1990, Cel. Mech. Dyn. Astron, 49, 347

Milani A., Knežević Z., 1994, Icarus, 107, 219

Milani A., Cellino A., Knežević Z., Novaković B., Spoto F., Paolicchi P., 2014, Icarus, 239, 46

Milani A., Spoto F., Knežević Z., Novaković B., Tsirvoulis G., 2016, in Chesley, S. R. and Morbidelli A, Jedicke, R. and Farnocchia, D., eds, Proc. IAU Symp. Vol. 318, Asteroids: New Observations, New Models., 28

Milani A., Knežević Z., Spoto F., Cellino A., Novaković B., Tsirvoulis G., 2017, Icarus, 288, 240

Morbidelli A., 1993, Icarus, 105, 48

Morbidelli A., Henrard J., 1991a, Cel. Mech. Dyn. Astron, 51, 131

Morbidelli A., Henrard J., 1991b, Cel. Mech. Dyn. Astron, 51, 169

Mothe-Diniz T., Roig F., Carvano J. M., 2005, Icarus, 174, 54

Nesvorný D., Brož M., Carruba V., 2015, in Michel P., DeMeo F. E., Bottke W. F., eds, Identification and Dynamical Properties of Asteroid Families, Asteroids IV, Univ. Arizona Press and LPI, Tucson, AZ, 297

Nobili A. M., Milani A., Carpino M., 1989, A&A, 210, 313

Sidlichovský M., Nervorný D., 1996, Cel. Mech. Dyn. Astron, 65, 137

Spoto F., Milani A., Knežević Z., 2015, Icarus, 257, 275

Tisserand F., 1882, Annales de l'Observatoire de Paris, 16, E.1

Williams J. G., 1969, PhD thesis. University of California, Los Angeles

Williams J. G., Faulkner J., 1981, Icarus, 46, 390

Yoshikawa M., 1987, Celestial Mechanics, 40, 233

Zappalà V., Cellino A., Farinella P., Knežević Z., 1990, AJ, 100, 2030

This paper has been typeset from a TeX/LaTeX file prepared by the author.